



RESEARCH ACTIVITIES

Life and Coordination-Complex Molecular Science

Department of Life and Coordination-Complex Molecular Science is composed of four divisions of Biomolecular science, two divisions of Coordination molecular science and two adjunct divisions. Biomolecular science divisions cover the studies on the elucidation of functions and mechanisms for various types of sensor proteins, protein folding, molecular chaperone, and metal proteins. Coordination complex divisions aim to develop molecular catalysts for the transformation of organic molecules, activation small inorganic molecules, and reversible conversion between chemical and electrical energies. Interdisciplinary alliances in the Department aim to create new basic concepts for the molecular and energy conversion through the fundamental science conducted at each division.

Bioinorganic Chemistry of Novel Hemeproteins

Department of Life and Coordination-Complex Molecular Science
Division of Biomolecular Functions



AONO, Shigetoshi
YOSHIOKA, Shiro
SAWAI, Hitomi
NISHIMURA, Muneto
TANIZAWA, Misako

Professor
Assistant Professor
JSPS Post-Doctoral Fellow
Graduate Student
Secretary

Heme-based sensor proteins show a novel function of the heme prosthetic group, in which the heme acts as the active site for sensing the external signal such as diatomic gas molecules and redox change. Aldoxime dehydratase is another novel hemeprotein, in which the heme prosthetic group tethers the substrate for its dehydration reaction. Our research interests are focused on the elucidation of the structure-function relationships of these novel hemeproteins.

1. Hydrogen Bonding Interaction on the Heme-Bound Ligand in the Heme-Based O₂ Sensor Protein¹⁾

HemAT is a signal transducer protein that is a member of methyl accepting chemotaxis proteins (MCPs), which is responsible for aerotaxis control of some bacteria and archaea. HemAT consists of two domains, the N-terminal sensor domain containing a heme and the C-terminal signaling domain that interacts with CheA, a component of CheA/CheY two-component system regulating the rotational direction of a flagellar motor in response to an input signal into MCPs. The heme in the sensor domain of HemAT acts as the active site for sensing its physiological effector, O₂. When O₂ binds to the

heme in the sensor domain, it is thought that a specific conformational change will occur, and then signal transduction will proceed from the sensor domain to the signaling domain. As a result, the self-kinase activity of CheA is regulated by a change in the interaction between HemAT and CheA via the specific conformational change of HemAT.

HemAT should discriminate O₂ from other gas molecules such as NO and CO, for which the heme environmental structure plays a crucial role. To elucidate the mechanism of selective O₂ sensing by HemAT, structural, mutagenesis, and spectroscopic studies were carried out for HemAT from *Bacillus subtilis* (HemAT-Bs). The interaction between the heme-bound ligand and the surrounding amino acid residue(s) plays a crucial role for selective sensing of O₂ and signal transduction by HemAT. In this work, we elucidated by resonance Raman spectroscopy how O₂ and CO interact with HemAT-Hs and HemAT-Rr, HemAT from *Halobacterium salinarum* and *Rhodospirillum rubrum*, respectively. HemAT-Hs and HemAT-Rr showed three conformers in the O₂-bound form, as is the case of HemAT-Bs, HemAT from *Bacillus subtilis*. Though the hydrogen bonding patterns observed in the three conformers were same among HemAT-Bs, HemAT-Hs, and HemAT-Rr, the involved residues for the hydrogen bonding interaction were different from one another.

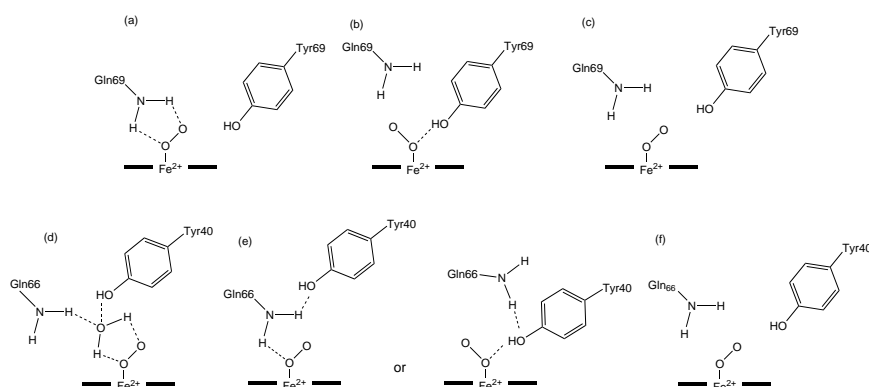


Figure 1. Hydrogen bonding network of the oxygen-bound form of HemAT-Hs (a-c) and HemAT-Rr (d-f).

2. Metal-Containing Sensor Proteins Sensing Diatomic Gas Molecules²⁾

All of the living organisms have a variety of regulatory systems to confront the change in the environmental conditions, which should be essential for maintaining the homeostasis in the cells, organs, and whole bodies. The chemical or physical stimuli act as signals for them to sense the change in the environmental conditions. These regulatory systems are responsible for the control of cell motility, gene expression, and/or enzymatic activity in response to the external stimuli. Sensing the external stimuli is the first step for these regulatory systems to work. Sensor (receptor) proteins should be required to sense these signals in biological systems, which sense the cognate signals in a specific manner.

Recently, it becomes apparent that diatomic gas molecules such as O₂, CO, and NO can act as signaling molecules for many biological processes. The functional role as external signals is a new one of these gas molecules in biological systems while it is well known that gas molecules are involved in biological systems as substrates and/or reaction products of many enzymatic reactions.

The gas sensor proteins usually use some prosthetic group to sense diatomic gas molecules. Heme, iron-sulfur cluster, and non-heme iron are known as the active center for these gas sensor proteins. When the gas sensor proteins sense their effector gas molecules, intramolecular and intermolecular signal transductions take place to regulate many physiological functions including gene expression, aerotaxis, and change in metabolic pathways, *etc.* The metal-containing prosthetic groups in these sensor proteins play a crucial role for selective sensing of their effectors.

In this perspective, I will discuss the structure and function of some O₂-, CO-, and NO-sensor proteins, especially focus on the structural, biochemical and biophysical properties of the active centers of these sensor proteins.

3. Protein Conformation Changes of HemAT-Bs upon Ligand Binding Probed by Ultraviolet Resonance Raman Spectroscopy³⁾

HemAT from *Bacillus subtilis* (HemAT-Bs) is a heme-based O₂ sensor protein that acts as a signal transducer responsible for aerotaxis. HemAT-Bs discriminates its physiological effector (O₂) from other gas molecules (CO and NO), although all of them bind to a heme. To monitor the conformational changes in the protein moiety upon binding of different ligands, we have investigated ultraviolet resonance Raman (UVRR) spectra of the ligand-free and O₂-, CO-, and NO-bound forms of full-length HemAT-Bs and several mutants (Y70F, H86A, T95A, and Y133F) and found that Tyr⁷⁰ in the heme distal side and Tyr¹³³ and Trp¹³² from the G-helix in the heme proximal side undergo environmental changes upon ligand binding. In addition, the UVRR results confirmed our previous model, which suggested that Thr⁹⁵ forms a hydrogen bond with heme-bound O₂, but Tyr⁷⁰ does not. It is deduced from this study that hydrogen bonds between Thr⁹⁵ and heme-bound O₂ and between His⁸⁶ and heme 6-propionate communicate the heme structural changes to the protein moiety upon O₂ binding but not upon CO and NO binding. Accordingly, the present UVRR results suggest that O₂ binding to heme causes displacement of the G-helix, which would be important for transduction of the conformational changes from the sensor domain to the signaling domain.

References

- 1) M. Nishimura, H. Yoshimura, K. Ozawa, S. Yoshioka, M. Kubo, T. Kitagawa and S. Aono, *J. Porphyrins Phthalocyanines* **12**, 142–148 (2008).
- 2) S. Aono, *Dalton Trans.* 3137–3146 (2008).
- 3) S. F. El-Mashtoly, Y. Gu, H. Yoshimura, S. Yoshioka, S. Aono and T. Kitagawa, *J. Biol. Chem.* **283**, 6942–6949 (2008).

Award

SAWAI, Hitomi; The best poster prize in 4th International Conference on Metals and Genetics (Paris, France, July 21–24, 2008).

Elucidation of the Molecular Mechanisms of Protein Folding

Department of Life and Coordination-Complex Molecular Science
Division of Biomolecular Functions



KUWAJIMA, Kunihiro	Professor
CHAUDHURI, Tapan K.	Visiting Associate Professor
MAKABE, Koki	Assistant Professor
MUKAIYAMA, Atsushi	IMS Fellow
VOLETY, Srinivas	Visiting Scientist; JSPS Invited Fellow
NAKAMURA, Takashi	Post-Doctoral Fellow
TAKAHASHI, Kazunobu	Graduate Student*
MIZUKI, Hiroko	Technical Fellow
ISOGAI, Miho	Secretary

Kuwajima group is studying mechanisms of *in vitro* protein folding and mechanisms of molecular chaperone function. Our goals are to elucidate the physical principles by which a protein organizes its specific native structure from the amino acid sequence. In this year, we studied the structure of the GroEL-GroES complex under physiological conditions by small-angle X-ray scattering, which is a powerful technique to directly observe the structure of the protein complex in solution.

1. Asymmetry of the GroEL-GroES Complex under Physiological Conditions as Revealed by Small-Angle X-Ray Scattering¹⁾

In spite of the well-known functional importance of GroEL-GroES complex formation during the chaperonin cycle, the stoichiometry of the complex has not been clarified. The complex can occur either as an asymmetric 1:1 GroEL-GroES complex or as a symmetric 1:2 GroEL-GroES complex,

although it remains uncertain which type is predominant under physiological conditions. To resolve this question, we studied the structure of the GroEL-GroES complex under physiological conditions by small-angle X-ray scattering, which is a powerful technique to directly observe the structure of the protein complex in solution. We evaluated molecular structural parameters, the radius of gyration and the maximum dimension of the complex, from the X-ray scattering patterns under various nucleotide conditions (3 mM ADP, 3 mM ATP γ S and 3 mM ATP in 10 mM MgCl₂ and 100 mM KCl) at three different temperatures (10 °C, 25 °C, and 37 °C). We then compared the experimentally observed scattering patterns with those calculated from the known X-ray crystallographic structures of the GroEL-GroES complex. The results clearly demonstrated that the asymmetric complex must be the major species stably present in solution under physiological conditions. On the other hand, in the presence of ATP (3 mM) and beryllium fluoride (10 mM NaF and 300 μ M BeCl₂), we observed the formation of a stable symmetric complex, suggesting the existence of a transiently formed symmetric complex during the chaperonin cycle.

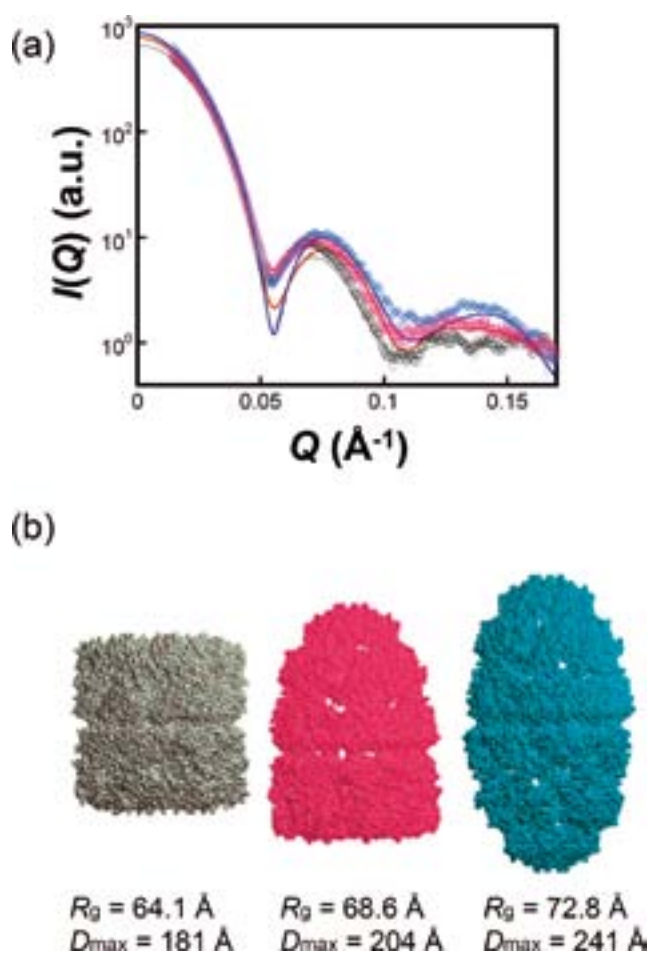


Figure 1. (a) Small-angle X-ray scattering patterns of molecular chaperones, GroEL and the GroEL-GroES complexes. (b) The three-dimensional structures of GroEL (gray), the bullet-type GroEL-GroES complex (magenta), and the football-type GroEL-GroES complex (cyan) (Inobe *et al.*, *Biophys. J.* **94**, 1392–1402 (2008)).

Reference

- 1) T. Inobe, K. Takahashi, K. Maki, S. Enoki, K. Kamagata, A. Kadooka, M. Arai and K. Kuwajima, *Biophys. J.* **94**, 1392–1402 (2008).

NMR Analyses of Structures, Dynamics, and Interactions of Biological Macromolecules

Department of Life and Coordination-Complex Molecular Science
Division of Biomolecular Functions



KATO, Koichi	Professor
SASAKAWA, Hiroaki	Assistant Professor*
YAMAGUCHI, Takumi	Assistant Professor
KAMIYA, Yukiko	IMS Fellow
SUGIHARA, Takahiro	Research Fellow
SUZUKI, Mariko	Research Fellow
UTSUMI, Maho	Graduate Student [†]
YOSHIKAWA, Sumi	Graduate Student [†]
NISHIO, Miho	Graduate Student [†]
TANAKA, Kei	Secretary

Our biomolecular studies are based on detailed analyses of structures and dynamics of various biological macromolecules and their complexes at atomic level, primarily using nuclear magnetic resonance (NMR) spectroscopy. In particular, we conducted studies aimed at elucidating dynamic structures of glycoconjugates and proteins for integrative understanding of the mechanisms underlying their biological functions. For this purpose, we use multidisciplinary approaches integrating the methodologies of molecular and cellular biology and nanoscience along with molecular spectroscopy. Here we report NMR studies of Fbs1, α -synuclein, group II chaperonin and prefoldin.

1. Molecular Recognition by Fbs1, an Intracellular Lectin Contributing to Quality Control of Glycoproteins¹⁾

Fbs1 is a cytosolic lectin putatively operating as a chaperone as well as a substrate-recognition subunit of the SCF^{Fbs1} ubiquitin ligase complex. To provide structural and functional basis of preferential binding of Fbs1 to unfolded glycoproteins, we herein characterize the interaction of Fbs1 with a heptapeptide carrying Man₃GlcNAc₂ by NMR spectroscopy and other biochemical methods. Inspection of the NMR data obtained by use of the isotopically labeled glycopeptide indicated that Fbs1 interacts with sugar-peptide junctions (Figure 1), which are shielded in native glycoprotein, in many cases, but become accessible to Fbs1 in unfolded glycoproteins. Furthermore, Fbs1 was shown to inhibit deglycosylation of denatured ribonuclease B by a cytosolic peptide:*N*-glycanase (PNGase). On the basis of these data, we suggest that Fbs1 captures malformed glycoproteins, protecting them from the attack of PNGase, during the chaperoning or ubiquitinating operation in the cytosol.

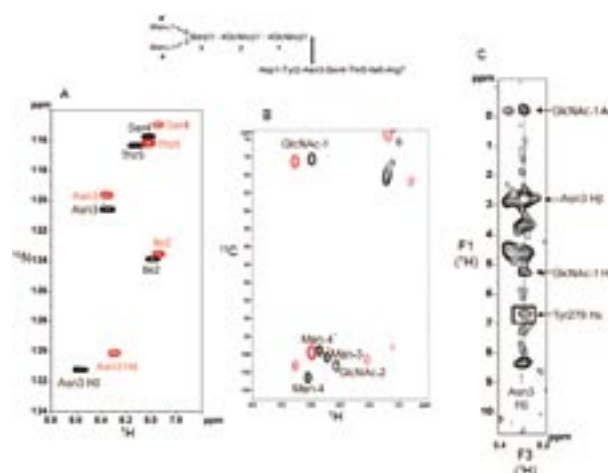


Figure 1. NMR spectra of the isotopically labeled heptapeptide carrying Man₃GlcNAc₂. (A) The anomeric region of ¹H-¹³C HSQC spectrum of the glycopeptides labeled with [¹³C₆]glucose and (B) amide region of ¹H-¹⁵N HSQC spectrum of the ¹⁵N-labeled glycopeptide in the presence (red) or absence (black) of equimolar amount of Fbs1-SBD. (C) Part of ¹⁵N-edited NOESY spectrum of the ¹⁵N-labeled glycopeptides bound to Fbs1-SBD (F₂(¹⁵N) = 129.6 ppm). The intermolecular NOE peak between Tyr279 H ϵ (Fbs1-SBD) and Asn3 H δ (glycopeptide) is boxed.

2. Antibody Binding and Site-Specific Phosphorylation of α -Synuclein, an Intrinsically Disordered Protein²⁾

Although biological importance of intrinsically disordered proteins is becoming recognized, NMR analyses of this class of proteins remain as tasks with more challenge because of poor chemical shift dispersion. It is expected that ultra-high field NMR spectroscopy offers improved resolution to cope with this difficulty. α -Synuclein, an intrinsically disordered protein, is identified as the major component of the Lewy bodies. Epitope mapping of an anti- α -synuclein monoclonal antibody and characterization of conformational effects of phosphorylation at Ser129 of α -synuclein were conducted

based on NMR spectral data collected at a 920 MHz proton frequency (Figure 2). These studies demonstrated that the employment of ultra-high field spectrometers is obviously advantageous for obtaining detailed information on conformations, modifications, and interactions of intrinsically disordered proteins in solution.

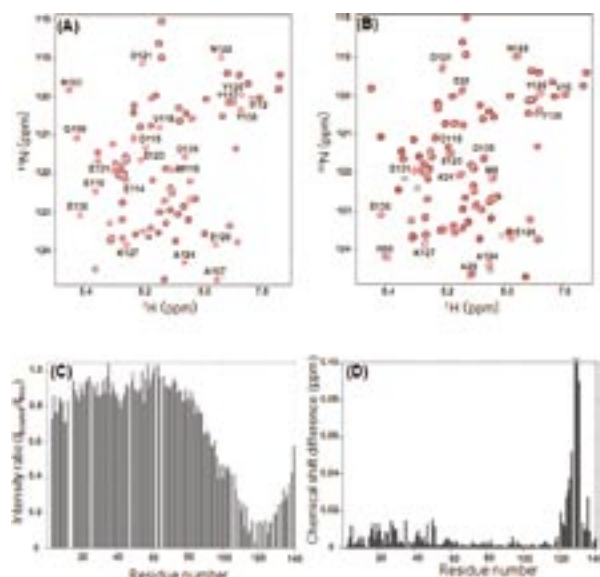


Figure 2. NMR analyses of antibody binding and phosphorylation of α -synuclein. ^1H - ^{15}N HSQC spectra of (A) [^{15}N] α -synuclein in the presence (black) and absence (red) of LB509 and (B) phosphorylated (black) and non-phosphorylated (red) [^{15}N] α -synuclein recorded at a proton frequency of 920 MHz. (C) Plot of the relative peak intensities, $I_{\text{bound}}/I_{\text{free}}$, of the HSQC cross peaks in the α -synuclein/LB509 complex and free α -synuclein versus the amino acid sequence of α -synuclein. (D) Profiles of chemical shift changes $[(\delta_{\text{N}}/5)^2 + \delta_{\text{H}}^2]^{1/2}$ upon phosphorylation at Ser129. Asterisks indicate the chemical shift differences are larger than 0.1 ppm for Ser129 (0.48 ppm) and E130 (0.20 ppm).

3. Dynamics of Group II Chaperonin and Prefoldin Probed by ^{13}C NMR Spectroscopy³⁾

Group II chaperonin (CPN) cooperates with prefoldin (PFD), which forms a jellyfish-shaped heterohexameric complex with a molecular mass of 87 kDa. PFD captures an unfolded protein with the tentacles and transfers it to the cavity of CPN. Although X-ray crystal structures of CPN and PFD have been reported, no structural information has been so far available for the terminal regions of the PFD tentacles nor for the C-terminal segments of CPNs, which were regarded to be functionally significant in the previous studies. We conducted ^{13}C NMR analyses on archaeal PFD, CPN and their complex, focusing on those structurally uncharacterized regions. The PFD and CPN complexes selectively labeled with ^{13}C at methionyl carbonyl carbons were separately and jointly sub-

jected to NMR measurements. ^{13}C NMR spectral data demonstrated that the N-terminal segment of the α and β subunits of PFD as well as the C-terminal segments of the CPN hexadecamer retain significant degrees of freedom in internal motion even in the complex with a molecular mass of 1.1 MDa (Figure 3).

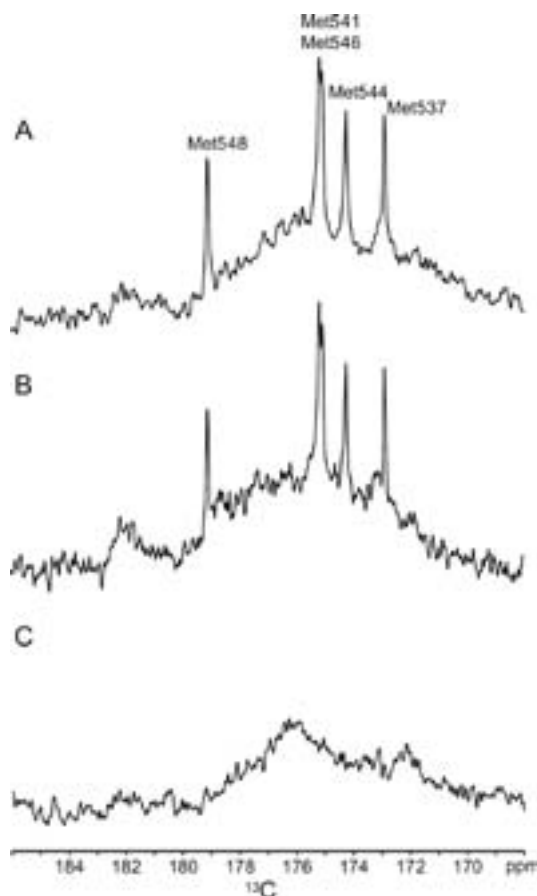


Figure 3. Hundred mega hertz ^{13}C NMR spectra of wild-type *Thermococcus* sp. strain KS-1 CPN (TKS α CPN) (A and B) and the truncated mutant of TKS α CPN that lacks the C-terminal 17 amino acid residues (C) labeled with [^{13}C]methionine in the absence (A and C) or presence (B) of 2 molar equivalent PFD. The proteins were dissolved in 50 mM Tris-HCl buffer, pH 8.0, containing 150 mM NaCl, 25 mM MgCl_2 , 0.02% NaN_3 , and 10% $^2\text{H}_2\text{O}$. The probe temperature was 45 $^\circ\text{C}$.

References

- 1) Y. Yamaguchi, T. Hirao, E. Sakata, Y. Kamiya, E. Kurimoto, Y. Yoshida, T. Suzuki, K. Tanaka and K. Kato, *Biochem. Biophys. Res. Commun.* **362**, 712–716 (2007).
- 2) H. Sasakawa, E. Sakata, Y. Yamaguchi, M. Masuda, T. Mori, E. Kurimoto, T. Iguchi, S. Hisanaga, T. Iwatsubo, M. Hasegawa and K. Kato, *Biochem. Biophys. Res. Commun.* **363**, 795–799 (2007).
- 3) E. Kurimoto, Y. Nishi, Y. Yamaguchi, T. Zako, R. Iizuka, N. Ide, M. Yohda and K. Kato, *Proteins: Struct., Funct., Bioinf.* **70**, 1257–1263 (2008).

* Present Address; JEOL Ltd. NMR/ESR team, Application & Research Group, Analytical Instrument Division, Akishima, Tokyo 196-8558

† carrying out graduate research on Cooperative Education Program of IMS with Nagoya City University

Structure-Function Relationship of Metalloproteins

Department of Life and Coordination-Complex Molecular Science
Division of Biomolecular Functions



FUJII, Hiroshi
KURAHASHI, Takuya
NONAKA, Daisuke
TAKAHASHI, Akihiro
TANIZAWA, Misako

Associate Professor
Assistant Professor
IMS Fellow
Graduate Student
Secretary

Metalloproteins are a class of biologically important macromolecules, which have various functions such as oxygen transport, electron transfer, oxidation, and oxygenation. These diverse functions of metalloproteins have been thought to depend on the ligands from amino acid, coordination structures, and protein structures in immediate vicinity of metal ions. In this project, we are studying the relationship between the electronic structures of the metal active sites and reactivity of metalloproteins.

1. Effect of a Tridentate Ligand on the Structure, Electronic Structure, and Reactivity of the Copper(I) Nitrite Complex: Role of the Conserved Three-Histidine Ligand Environment of the Type-2 Copper Site in Copper-Containing Nitrite Reductases¹⁾

It is postulated that the copper(I) nitrite complex is a key reaction intermediate of copper containing nitrite reductases (Cu-NiRs), which catalyze the reduction of nitrite to nitric oxide (NO) gas in bacterial denitrification. To investigate the structure-function relationship of Cu-NiR, we prepared five new copper(I) nitrite complexes with sterically hindered tris(4-imidazolyl)carbinols [Et-TIC: tris(1-methyl-2-ethyl-4-imidazolyl)carbinol and *i*Pr-TIC: tris(1-methyl-2-isopropyl-4-imidazolyl)carbinol] or tris(1-pyrazolyl)methanes [Me-TPM: tris(3,5-dimethyl-1-pyrazolyl)methane, Et-TPM: tris(3,5-diethyl-1-pyrazolyl)methane, and *i*Pr-TPM: tris(3,5-diisopropyl-1-pyrazolyl)methane]. The X-ray crystal structures of all of these copper(I) nitrite complexes were mononuclear η^1 -



Figure 1. Structure of Active Site Model Complex of Copper Nitrite Reductase (left) and its Electron Density of the HOMO (right).

N-bound nitrite complexes with a distorted tetrahedral geometry. The electronic structures of the complexes were investigated by absorption, MCD, NMR and vibrational spectroscopy. All of these complexes are good functional models of Cu-NiR that form NO and copper(II) acetate complexes well from reactions with acetic acid under anaerobic conditions. A comparison of the reactivity of these complexes, including previously reported (*i*Pr-TACN)Cu(NO₂), *i*Pr-TACN: 1,4,7-triisopropyl-1,4,7-triazacyclononane, clearly shows the drastic effects of the tridentate ligand on Cu-NiR activity. The copper(I) nitrite complex with the Et-TIC ligand, which is similar to the highly conserved three-histidine ((His)₃) ligand environment in the catalytic site of Cu-NiR, had the highest Cu-NiR activity. This result suggests that the (His)₃ ligand environment is essential for acceleration of the Cu-NiR reaction. The highest Cu-NiR activity for the Et-TIC complex can be explained by the structural and spectroscopic characterizations and the molecular orbital calculations presented in this paper. Based on these results, the functional role of the (His)₃ ligand environment in Cu-NiR is discussed.

2. Transient Intermediates from Mn(salen) with Sterically-Hindered Mesityl Groups: Interconversion between Mn^{IV}-Phenolate and Mn^{III}-Phenoxy Radical as an Origin for Unique Reactivity²⁾

In order to reveal structure-reactivity relationships for the high catalytic activity of the epoxidation catalyst Mn(salen), transient intermediates are investigated. Steric hindrance incorporated to the salen ligand enables highly selective generation of three related intermediates, O=Mn^{IV}(salen), HO-Mn^{IV}(salen) and H₂O-Mn^{III}(salen⁺), each of which is thoroughly characterized using various spectroscopic techniques including UV-vis, EPR, resonance Raman, ESI-MS, ²H-NMR and X-ray absorption spectroscopy. These intermediates are all one-electron oxidized from the starting Mn^{III}(salen) precursor, but differ only in the degree of protonation. However, structural and electronic features are strikingly different: The Mn–O bond length of HO-Mn^{IV}(salen) (1.83 Å) is considerably longer than that of O=Mn^{IV}(salen) (1.58 Å); the electronic configuration of H₂O-Mn^{III}(salen⁺) is Mn^{III}-phenoxy radical, while those of O=Mn^{IV}(salen) and HO-Mn^{IV}(salen) are Mn^{IV}-phenolate. Among O=Mn^{IV}(salen), HO-Mn^{IV}(salen) and H₂O-Mn^{III}(salen⁺), only the O=Mn^{IV}(salen) can transfer oxygen to phosphine and sulfide substrates, as well as abstract hydrogen from weak C–H bonds, although the oxidizing power is not enough to epoxidize olefins. The high activity of Mn(salen) is a direct consequence of the favored formation of the reactive O=Mn^{IV}(salen) state.

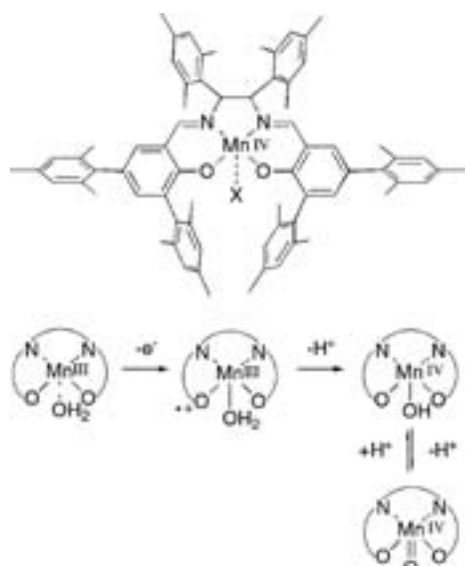


Figure 2. Structure of Manganese(IV) Salen Complex synthesized in this study (upper) and protonation and deprotonation of Mn(IV)=O(Salen) complex (bottom).

3. Chiral Distortion in a Mn^{IV}(salen)(N₃)₂ Derived from Jacobsen's Catalyst as a Possible Conformation Model for its Enantioselective Reactions³⁾

The Mn^{IV}(salen)(N₃)₂ complex (**3**) from Jacobsen's catalyst is synthesized, and the X-ray crystal structures of **3** as well as the starting Mn^{III}(salen)(N₃)(CH₃OH) complex (**2**) are determined in order to investigate the conformation of the high-valent Mn^{IV}(salen) molecule in comparison with that of Mn^{III}(salen). The asymmetric unit of the crystal of **3** contains four complexes, all of which adopt a nonplanar stepped conformation effectively distorted by the chirality of the diimine bridge. The asymmetric unit of **2** also contains four complexes. Two of them show a stepped conformation of a lesser degree, but the other two adopt a bowl-shaped conformation. Comparison of the structural parameters shows that the Mn center in **3** is coordinated from both sides by two external axial N₃ ligands with significantly shorter bond length, which could induce greater preference for the stepped conformation in **3**. The CH₃CN solution of **3** shows circular dichroism with a significantly strong band at 275 nm as compared to **2**, suggesting that **3** may adopt a more chirally-distorted conformation also in solution. The circular dichroism spectrum of **3** is slightly altered with isodichroic points from 298 to 253 K, and shows no further change at temperatures lower than 253 K, suggesting that the solution of **3** contains equilibrium between two conformers, where a low-energy conformer with more chiral distortion is predominantly favored even at room temperature. **2** and **3** are thoroughly characterized using various techniques including cyclic voltammetry, magnetic susceptibility, UV-vis, electron paramagnetic resonance, ¹H NMR, infrared spectroscopy and electrospray ionization mass spectrometry.

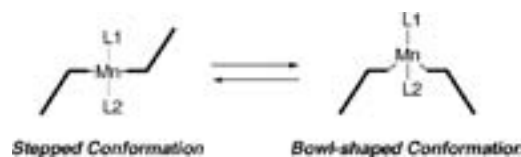


Figure 3. Equilibrium between stepped and bowl-shaped conformations of Mn(salen), which is directed by the position of the Mn center from the basal N₂O₂ ligand plane.

References

- 1) M. Kujime, C. Izumi, T. Tomura, M. Hada and H. Fujii, *J. Am. Chem. Soc.* **130**, 6088–6098 (2008).
- 2) T. Kurahashi, A. Kikuchi, T. Tosha, Y. Shiro, T. Kitagawa and H. Fujii, *Inorg. Chem.* **47**, 1674–1686 (2008).
- 3) T. Kurahashi and H. Fujii, *Inorg. Chem.* **47**, 7556–7567 (2008).

Fabrication of Silicon-Based Planar Ion-Channel Biosensors and Integration of Functional Cell Membrane Model Systems on Solid Substrates

Department of Life and Coordination-Complex Molecular Science
Division of Biomolecular Sensing



URISU, Tsuneo
TERO, Ryugo
MAO, Yangli
KIM, Yong-Hoon
CHIANG, Tsung-Yi
ZHANG, Zhen-Long
UNO, Hidetaka
SAYED, Abu
NAKAI, Naohito
ASANO, Toshifumi
SHANG, Zhi-Guo
FUJIWARA, Kuniyo
SHIMIZU, Atsuko

Professor
Assistant Professor
IMS Fellow
Research Fellow
Research Fellow
Graduate Student
Graduate Student
Graduate Student
Graduate Student
Graduate Student
Graduate Student
Secretary

We are interested in the investigation of cell membrane surface reactions and the pathogen mechanism of the neurodegenerative diseases, based on the molecular science. We are advancing two subjects, aiming the creation and development of new molecular science field, “medical molecular science.” One is the development of ion channel biosensor and its application to the neural network analyzer device. The other is the fundamental understanding of bilayer membrane properties using the artificial lipid bilayers on solid substrates, which is called supported bilayers, by means of atomic force microscope and fluorescence microscope-based techniques.

1. The Morphology of $\text{GM1}_x/\text{SM}_{0.6-x}/\text{Chol}_{0.4}$ Planar Bilayers Supported on SiO_2 Surfaces¹⁾

Ganglioside GM1 (GM1), sphingomyelin (SM) and cholesterol (Chol) are dominant lipid components of rafts in plasma membranes. The morphology of supported planar bilayers composed of GM1, SM and Chol (Figure 1) on SiO_2 surfaces has been studied by atomic force microscopy and fluorescence microscopy. The component ratio of the SPB ($\text{GM1}_x/\text{SM}_{0.6-x}/\text{Chol}_{0.4}$) was varied in the range of $x = 0-0.25$.

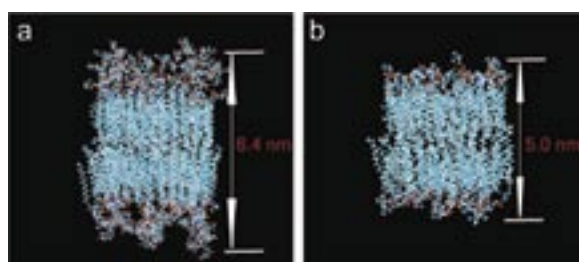


Figure 1. Membrane structure of (a) GM1/SM/Chol (1:2:2 molar ratio) and (b) SM/Chol (1:1 molar ratio) obtained by MD simulation.

The unique changes in morphology depending on the GM1 concentrations (Figure 2) are qualitatively explained by hydrogen bonding and the hydrophobic interactions between SM and Chol, and by hydrogen bonding and the steric effects between bulky GM1 headgroups under Ca^{2+} existing conditions and the electrostatic repulsion between the negative charges of GM1 headgroups under Ca^{2+} nonexisting conditions.

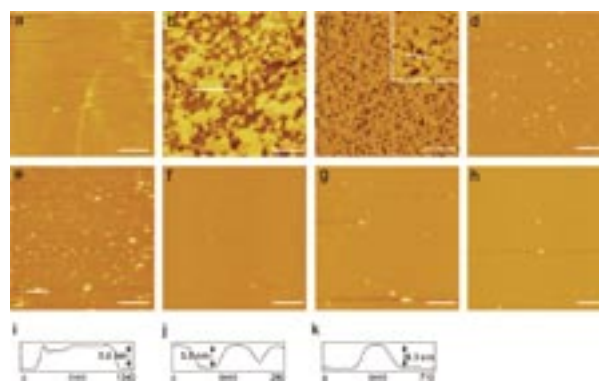


Figure 2. AFM images and line profiles of $\text{GM1}_x/\text{SM}_{0.6-x}/\text{Chol}_{0.4}$ SPBs formed on SiO_2 surface in a buffer solution containing Ca^{2+} with different GM1 content (molar ratio): (a) $x = 0$, (b) $x = 0.05$, (c) $x = 0.1$ (insert is magnified image ($1.0 \times 1.0 \mu\text{m}^2$)), (d) $x = 0.15$, (e) $x = 0.2$, and (f) $x = 0.25$. Also, AFM images of $\text{GM1}_x/\text{SM}_{0.6-x}/\text{Chol}_{0.4}$ SPBs formed without Ca^{2+} : (g) $x = 0.1$ and (h) $x = 0.2$. (i), (j), and (k) correspond to line profiles along white lines of (b), (c), and (e). Scale bar is $1.0 \mu\text{m}$.

2. Lipid Bilayer Membrane with Atomic Step Structure: Supported Bilayer on Step-and-Terrace $\text{TiO}_2(100)$ Surface²⁾

Formation of a supported planar lipid bilayer (SPLB) and

its morphology on step-and-terrace rutile-TiO₂(100) surfaces were investigated by fluorescence microscopy and atomic force microscopy. The TiO₂(100) surfaces consisting of atomic steps and flat terraces were formed on a rutile-TiO₂ single crystal wafer by a wet-treatment and annealing under oxygen flow. Intact vesicular layer formed on the TiO₂(100) surface when the surface was incubated in a sonicated vesicle suspension in the condition that a full-coverage SPLB forms on SiO₂, as reported in previous studies. However a full-coverage, continuous and fluid SPLB was obtained on the step-and-terrace TiO₂(100) depending on the lipid concentration, incubation time and vesicle size. The SPLB on the TiO₂(100) also has the step-and-terrace morphology following the substrate structure precisely even though the SPLB is in the fluid phase and ~1 nm thick water layer exists between the SPLB and the substrate. This membrane distortion on the atomic scale affects the phase separation structure of a binary bilayer in micrometer order (Figure 3). The interaction energy calculated including DLVO and non-DLVO factors shows that a lipid membrane on the TiO₂(100) gains 20 times larger energy than on SiO₂. This specifically strong attraction on TiO₂ makes the fluid SPLB precisely follow the substrate structure of angstrom order.

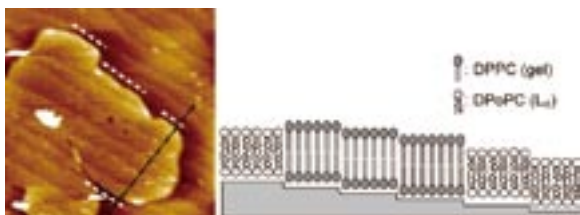


Figure 3. AFM topograph ($2.0 \times 2.0 \mu\text{m}^2$) of the DPPC+DPoPC binary SPLB. The gel-phase domain edges running along the substrate steps are indicated by white dashed lines. The schematic illustration shows the cross-sectional view perpendicular to the substrate steps, like the black dashed-dotted line in the AFM image.

3. New Infrared Reflection Absorption Spectroscopy System for in-situ Observation of Adsorbed Biomaterials on Solid Surfaces under Water

In situ under water infrared reflection absorption spectroscopy (IRRAS) is an attractive vibration spectroscopy for biomaterials adsorbed on the IR non-transparent materials such as gold substrates, which are important in many biosensors and biochips such as DNA chips and surface plasmon resonance (SPR). We have constructed a new IRRAS system in which the sample solution is confined in the narrow space between CaF₂ prism surface and the substrate surface, and the IR beam is directed onto the substrate surface passing through the prism. The sample holders are designed to keep the thickness highly constant between the prism surface and the substrate surface during the measurements. It is essentially important, in the present system, to make sure of the condition that sample proteins are adsorbed on the substrate surface but

not on the prism surface. The quite different condition in this point between fibronectin (FN) and immunoglobulin G (IgG) was well explained by the charge of the amino acid residue and the salt effects. Clear amide I bands were successfully observed under water for FN adsorbed on the SiO₂ surface (Figure 4a) and IgG on the gold surface (Figure 4b).

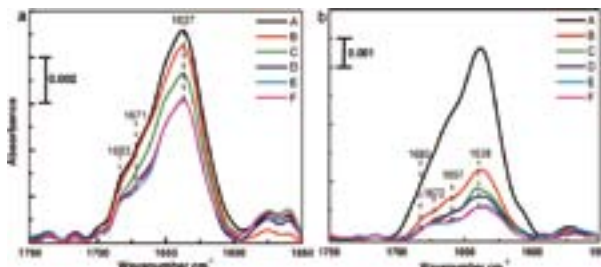


Figure 4. Amide I bands of adsorbed proteins on the substrate surfaces observed by in-situ IRRAS under D₂O solution. a) Spectra of FN using pure D₂O as the solvent; A, B, C, D, E and F. b) Spectra of IgG using NaCl (140 mM) added D₂O based PBS solution; A, B, C, D, E and F. A) Spectra for protein injection and waiting 3 h (FN) and 1h (IgG) for adsorption on solid surface. Spectra were taken every after 0.5 ml D₂O solution flushes; B) 0.50 ml C) 1.0 ml D) 1.5ml E) 2.0 ml F) 2.5 ml.

4. Development of Cell Culture Type Planar Ion Channel Biosensor for Nerve Cell Signaling Analysis³⁾

We have developed a new planar ion channel biosensor with cell culture function using SOI (Silicon On Insulator) substrate. This sensor enables not only the miniaturization of the sensor size and the high throughput screening application, but also is capable of the long time and the time lapse measurements that are difficult in the conventional any planar and pipette patch-clamp methods. The surface of SOI substrate was coated by patterned extracellular matrix (ECM), such as fibronectin and poly-L-lysine, to promote the cell adhesion and control the growth area at the preliminary designed position. TRPV1 (Transient receptor potential vanilloid type 1) channel-expressing single HEK293 cell was positioned on the micropore of the SOI substrate. Whole-cell arrangement was formed by the perforated patch using nystatin. The ion channel current was successfully measured by capsaicin stimulations. Experiments using mouse cerebral cortex cell is now under way.

References

- 1) Y. Mao, R. Tero, Y. Imai, T. Hoshino and T. Urisu, *Chem. Phys. Lett.* **460**, 289–294 (2008).
- 2) R. Tero, T. Ujihara and T. Urisu, *Langmuir* **24**, 11567–11576 (2008).
- 3) Z. L. Zhang, T. Asano, H. Uno, R. Tero, M. Suzui, S. Nakao, T. Kaito, K. Shibasaki, M. Tominaga, Y. Utsumi, Y. L. Gao and T. Urisu, *Thin Solid Films* **516**, 2813–2815 (2008).

Development of Fluorescent and Bioluminescent Proteins for Imaging Biomolecules

Department of Life and Coordination-Complex Molecular Science
Division of Biomolecular Sensing



OZAWA, Takeaki	Associate Professor*
TAKEUCHI, Masaki	Assistant Professor
HIDA, Naoki	IMS Fellow
MUHAMMAD, Awais	Post-Doctoral Fellow

Current focus on biological research is to quantify and visualize biomolecules in living cells and animals. To probe biomolecular functions and dynamics, we are exploring a new way for developing fluorescent and bioluminescent reporter proteins based on protein splicing and complementation techniques. The reporter proteins can be utilized to development of analytical methods for detecting protein–protein interactions, intracellular localization of proteins and their dynamics, enzyme activities, gene expression and production of small biomolecules.

1. Development of Multicolor Bioluminescent Probes for Protein–Protein Interactions in Living Subjects

Bimolecular complementation using luminescent proteins has a potential to perform reversible and multiplex detection of protein–protein interactions in opaque or auto-fluorescent living subjects. We constructed multicolor luciferase fragments, of which sensitivity and signal-to-background ratio were considerably improved by using an engineered carboxy-terminal fragment of a click beetle luciferase and amino-terminal fragments of luciferases with different spectral characteristics. We investigated complementation of split luciferases from firefly (PpyLuc), click beetle in green (ELuc) and click beetle in red (CBRLuc). The N- and C-terminal fragments were fused to FK506-binding protein (FKBP) and FKBP-binding domain (FRB). A pair of the fusion proteins was co-expressed in mammalian cells and the luminescence intensities

were examined by a luminometer. Amino- and carboxy-fragments of individual luciferase were found complement enough to recover the bioluminescence upon interaction between FKBP and FRB in the presence of rapamycin. But, no cross complementation was detected when combination of different luciferase fragments was used. To make cross complementation possible, a new C-terminal fragment that has an ability to complement multiple N-terminal fragments was developed by the random mutagenesis. A mutant of the C-terminal fragment including three point mutations (mCLuc1) showed most remarkable properties, which enabled complement to all the N-terminal fragments of PpyLuc, CBR and ELuc. The signal-to-background ratio upon using mCLuc1 was improved higher than that of the native one. The competitive inhibitor FK506 prevented rapamycin-induced luciferase activity generated by mCLuc1 and N-terminal PpyLuc, confirming that their complementation is reversible. Thus, mCLuc1 allowed new complementation partners of all the N-terminal luciferases, which can be widely used for monitoring protein-protein interactions in living cells.

2. Bioluminescence Imaging of Kinase-Induced Interactions Among Bad, 14-3-3, and Bcl-2 in Living Mice

To demonstrate the applicability of the complementation of multicolor split luciferases in mammals, we used three proteins of Bad, 14-3-3 and Bcl-2, which are known to regulate cell survival. In the presence of growth factors, Bad is phos-

phorylated, thereby interacting with the 14-3-3 protein. Upon deprivation of growth factors, Bad is dephosphorylated and consequently, binds to Bcl-2. The Bad protein was fused to McLuc1, while the 14-3-3 and Bcl-2 proteins were fused to N-terminal fragments of ELuc and PpyLuc, respectively. The fusion constructs were co-transfected into COS-7 cells and photon counts were evaluated. A strong intensity of bioluminescence was obtained from the cells including Bad and 14-3-3 proteins, indicating that Bad interacts 14-3-3 endogenously. To confirm that the increase in the luminescence signal was indeed triggered by the interaction of Bad and 14-3-3, we constructed Bad mutants in which several serine residues were replaced by alanine. These serine residues are necessary for interaction of Bad with 14-3-3. The luminescence signals were significantly reduced upon expression of 14-3-3 with these Bad mutants in the cells. We next used the same construct of Bad-McLuc1 for the analysis of interaction with Bcl-2. Strong bioluminescence was obtained upon over-expression of Bad-McLuc1 and Bcl-2 connected with N-terminal PpyLuc in COS-7 cells. Addition of Bcl-2 inhibitors resulted in reducing the luminescence, demonstrating that three fragments of McLuc1, N-terminal ELuc and PpyLuc can be used for detecting interactions of a protein associated with multiple distinct protein partners.

3. Bioluminescence Imaging of Kinase-Induced Interaction of pSmad1-Smad4 in *Xenopus laevis* Embryo

To evaluate usefulness of the reversible and high-sensitive complementation analysis with McLuc1, we used a heteromeric complex between Smad1 and Smad4 involved in cytoplasmic signaling of the bone morphogenetic protein (BMP) in a *Xenopus laevis* embryo. The embryo has a large amount of fluorescent yolk, which often hampers fluorescence imaging. We constructed a set of probes consisting of Smad1 connected with N-terminal PpyLuc and Smad4 connected with McLuc1. The probes were expressed in COS-7 cells containing either constitutive active form of transmembrane receptor (ALK3), or its dominant negative form (DL). The cells expressing ALK3 resulted in a strong luminescence in comparison to the cells expressing DL receptor or mock-transfected cells. A Smad1 mutant lacking phosphorylation sites showed negligible luminescence, indicating that the phosphorylated Smad1 interacted with Smad4, thereby resulting in complement of the luciferase fragments in living cells. Next, we synthesized mRNA from each cDNA construct of the probes and micro-injected into the cell embryo. The embryonic development was monitored under the fluorescence microscope equipped with a

CCD camera. From an early stage, a weak but significant signal of luminescence started to be detected in the trunk region of neural tube, and thereafter the signal became intense along the entire neural tube from head to tail. The signal was sustained up for a while, but changed faint gradually, indicating dissociation between Smad1 and Smad4. These results demonstrate that bioluminescence complementation imaging using the McLuc1 and N-terminal PpyLuc enabled spatial and temporal imaging of protein-protein interactions acting on the endogenous cellular signaling in living *Xenopus* embryos.

4. A Genetically Encoded Luminescent Indicator for Detecting Intracellular Cyclic GMP in Living Cells and Plants

In order to quantify and image cellular signaling processes in living cells and subjects, we developed a new analytical method using a luciferase. The principle is based on intramolecular complementation of the split fragments of luciferase. The split fragments of luciferase are fused to a cGMP-binding domain of phosphodiesterase (PDE). When concentration of cGMP increases in cytosol, interaction of cGMP with its binding domain of PDE causes a conformational change in the domain structure. The amino- and carboxyl-terminal fragments of luciferase are brought to come together, and full-length luciferase is reconstituted thereafter. After this luminescent indicator for cGMP was transiently expressed in HEK293 cells, a membrane permeable cGMP analog or a chemical (sodium nitroprusside) was added to the cell lysates or the living cells in the presence of luciferin. We found that luminescence intensities increased with increasing concentrations of the chemicals, which were detected by a luminometer or luminescent microscope. When the indicator was transiently expressed in *Arabidopsis* cells, chemicals that induce salt or osmotic stress were added to the cell lysates or the living cells. We also detected increases in the luminescence intensities upon stimulating stress-inducing chemicals. Thus, we demonstrated quantitative detection and imaging of ligand-induced increases of cGMP in living cells and plants.

References

- 1) T. Ozawa and Y. Umezawa, *Methods Mol. Biol.* **390**, 269–280 (2007).
- 2) T. Ozawa and Y. Umezawa, *Methods Mol. Biol.* **390**, 119–130 (2007).
- 3) C. Wei, M. Yamoto, W. Wei, Z. Zhao, K. Tsumoto, T. Yoshimura, T. Ozawa and Y. J. Chen, *Med. Clin. North Am.* **91**, 889–898 (2007).

Heterogeneous Catalytic Systems for Organic Chemical Transformations in Water

Department of Life and Coordination-Complex Molecular Science
Division of Complex Catalysis



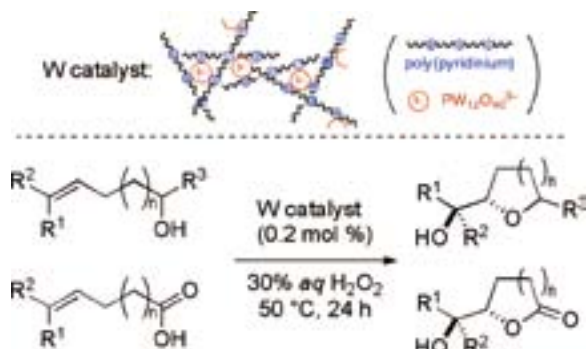
UOZUMI, Yasuhiro
YAMADA, Yoichi M. A.
OSAKO, Takao
OE, Yohei
HAMASAKA, Go
MATSUJURA, Yutaka
TAKENAKA, Hiroe
HIRAI, Yoshinori
BEPPU, Tomohiko
WATANABE, Toshihiro
KOBAYASHI, Noboru
TORII, Kaoru
SASAKI, Tokiyo
TANIWAKE, Mayuko

Professor
Assistant Professor*
Assistant Professor
IMS Fellow[†]
IMS Fellow
Post-Doctoral Fellow
Research Fellow
Research Fellow
Graduate Student
Graduate Student
Graduate Student
Technical Fellow
Secretary
Secretary

Various organic molecular transformations catalyzed by transition metals were achieved under heterogeneous aqueous conditions by use of amphiphilic resin-supported metal complexes or convoluted polymeric metal catalysts which were designed and prepared by this research group. In particular, highly stereoselective asymmetric π -allylic substitution and oxidative cyclization, both of which were performed in water under heterogeneous conditions with high recyclability of the polymeric catalysts, are highlights among the achievements of the 2007–2008 period to approach what may be considered ideal chemical processes of next generation. Representative results are summarized hereunder.

1. Development of Tightly Convoluted Polymeric Phosphotungstate Catalysts and Their Application to Oxidative Cyclization of Alkenols and Alkenoic Acids¹⁾

Tightly convoluted polymeric phosphotungstate catalysts were prepared via ionic-assembly of $H_3PW_{12}O_{40}$ and poly(alkylpyridinium)s. An oxidative cyclization of various alkenols and alkenoic acids was efficiently promoted by the poly-

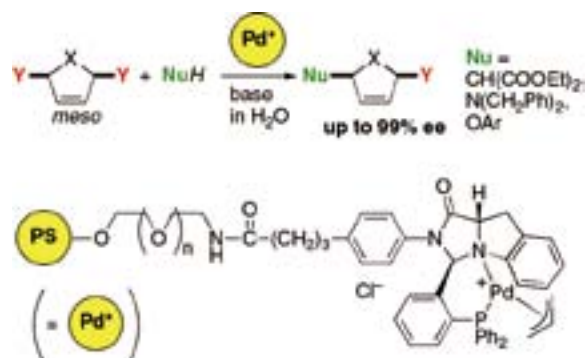


Scheme 1. Oxidative Cyclization of Alkenyl Alcohols and Alkenoic Acids with a Convoluted Polymeric Phosphotungstate.

meric phosphotungstate catalyst in *aq.* H_2O_2 in the absence of organic solvents to afford the corresponding cyclic ethers and lactones in high yield. The catalyst was reused four times without loss of catalytic activity. The polymeric phosphotungstate was unambiguously characterized by spectro- and microscopic studies (MAS $^{31}P\{^1H\}$ NMR, IR spectroscopy, elemental analysis, TEM, SEM, and EDS).

2. Allylic Substitution of *meso*-1,4-Diacetoxycycloalkenes in Water with an Amphiphilic Resin-Supported Chiral Palladium Complex³⁾

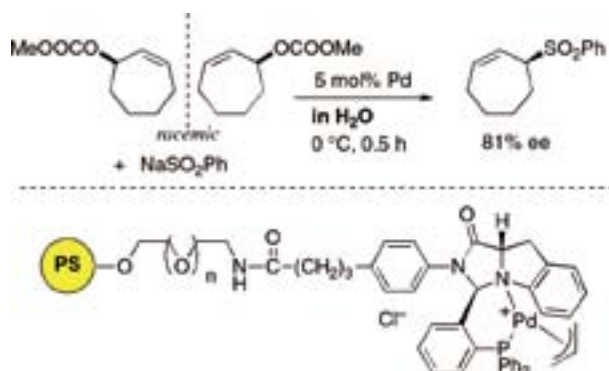
Asymmetric π -allylic substitution of *meso*-1,4-diacetoxycyclopentene and *meso*-1,4-diacetoxycyclohexene with various nucleophiles was performed with an amphiphilic polystyrene-poly(ethylene glycol) (PS-PEG) resin-supported chiral imidazoindole phosphine-palladium complex in water as a single reaction medium under heterogeneous conditions to give the corresponding 1-acetoxy-4-substituted cycloalkenes with up to 99% ee.



Scheme 2. Enantioselective Desymmetrization of *meso*-Cycloalkenyl Diacetate in Water with an Amphiphilic Resin-Supported Complex.

3. π -Allylic Sulfonation in Water with Amphiphilic Resin-Supported Palladium-Phosphine Complexes⁴⁾

π -Allylic substitution of allyl esters with sodium arylsulfinate was performed with an amphiphilic polystyrene-poly(ethylene glycol) (PS-PEG) resin-supported phosphine-palladium complex in water as a single reaction medium under heterogeneous conditions to give allyl sulfones in good to high yields. Catalytic asymmetric allylic substitution of cycloalkenyl esters also took place in water using a PS-PEG resin-supported chiral imidazoindolephosphine-palladium complex to give cycloalkenyl sulfones with up to 81% ee.



Scheme 3. Enantioselective Sulfonation of Cycloalkenyl Esters in Water with an Amphiphilic Resin-Supported Complex.

4. Highly Efficient Heterogeneous Aqueous Kharasch Reaction with an Amphiphilic Resin-Supported Ruthenium Catalyst⁵⁾

An amphiphilic polystyrene-polyethylene glycol (PS-PEG) resin-supported ruthenium complex was designed and pre-

pared. The polymeric Ru complex was found to promote the transition metal-catalyzed atom transfer radical addition of halogenated compounds to olefins, the Kharasch reaction, in water under heterogeneous as well as AIBN-free conditions with a high level of atom-economy to meet green chemical requirements.



Scheme 4. Kharasch Reaction in Water with an Amphiphilic Resin-Supported Ruthenium Complex.

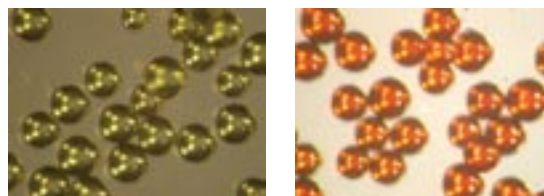


Figure 1. Microscopic Images of PS-PEG-NHCO-C₆H₄-PPh₂ (left) and PS-PEG-NHCO-C₆H₄-PPh₂-RuCpCl₂ (right).

References

- 1) Y. M. A. Yamada and Y. Uozumi, *Tetrahedron* **63**, 8492–8498 (2007).
- 2) Y. Uozumi, *Pure Appl. Chem.* **79**, 1481–1489 (2007).
- 3) Y. Uozumi, H. Takenaka and T. Suzuka, *Synlett* 1557–1561 (2008).
- 4) Y. Uozumi and T. Suzuka, *Synthesis* 1960–1964 (2008).
- 5) Y. Oe and Y. Uozumi, *Adv. Synth. Catal.* **350**, 1771–1775 (2008).

Award

YAMADA, Yoichi M. A.; The Commendation for Science and Technology by the Minister of Education, Culture, Sports, Science and Technology: The Young Scientists' Prize 2008.

* Present Address; RIKEN, Wako, Saitama 351-0198

† Present Address; Doshisha University, Kyotanabe, Kyoto 610-0321

Synthesis of Metal Complexes Aiming to Convert between Chemical Energy and Electrical One

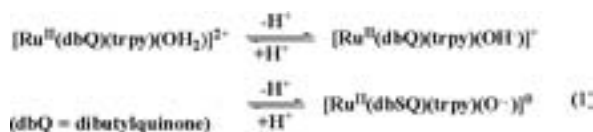
Department of Life and Coordination-Complex Molecular Science
Division of Functional Coordination Chemistry



TANAKA, Koji
WADA, Tohru
OZAWA, Hironobu
KOSHIYAMA, Tamami
FUKUSHIMA, Takashi
TSUKAHARA, Yuhei
YAMAGUCHI, Yumiko
NAKAGAKI, Shizuka

Professor
Assistant Professor
IMS Fellow
Post-Doctoral Fellow
Post-Doctoral Fellow
Graduate Student
Secretary
Secretary

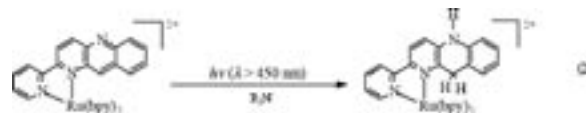
Metal ions involved in various metal proteins play key roles to generate metabolic energies through redox reactions of organic molecules. Metal complexes that have an ability to oxidize organic molecules at potentials more negative than reduction of dioxygen are feasible energy converter between chemical energy and electrical one. Some of high valent Ru=O complexes obtained by sequential proton and electron loss of the corresponding aqua-Ru complexes are proven to be active for the oxidation of organic molecules. However, the oxidation potentials of those aqua complexes to prepare high valent Ru=O ones are too positive to use as an energy transducer. We have succeeded smooth conversion from aqua to oxo ligands on Ru-dioxolene framework through proton coupled intramolecular electron transfer from the deprotonated form of the Ru–OH moiety to the dioxolene ligand (eq 1). The aqua-oxo



conversion using the unique redox behavior of Ru–dioxolene frameworks allowed us to isolate an unprecedented metal-oxo radical complex.

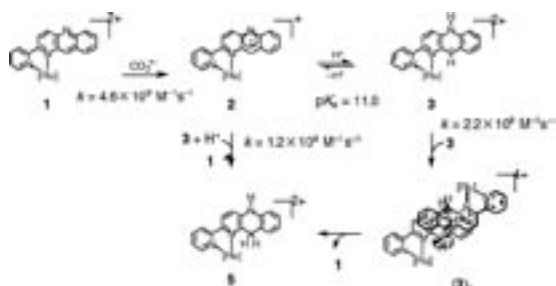
In addition to elucidation of the reactivity of Ru-oxyl radical complexes as electrocatalysts toward the oxidation of organic molecules, we are also aiming to develop multi-electron reduction of small inorganic molecules such as CO₂, N₂, and H₂O under mild reactions conditions, which would be key reactions to construct a renewable society. The difficulty in reductive activation of those molecules is attributable to the undesirable formation of high energy intermediates that are produced during stepwise one-electron transfer to the reaction centers. Recently, we showed that a mononuclear [Ru^{II}(pbn)(bpy)₂]²⁺ (bpy = 2,2'-bipyridine, pbn = 2-(2-pyridyl)benzo[b]-1,5-naphthyridine) ([1]²⁺) is smoothly converted to [Ru(pbnH₂)(bpy)₂]²⁺ ([1HH]²⁺) by not only electrochemical but also

photochemical reductions in the presence of proton (eq 2). Furthermore, the resultant [Ru(pbnH₂)(bpy)₂]²⁺ works as a functional model as the nicotinamide adenine dinucleotide NAD⁺/NADH redox reaction that plays a key role in a reservoir/source of two electrons and one proton in various biological energy transfer systems.



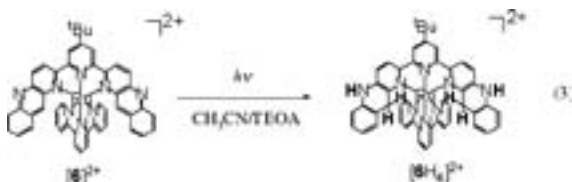
1. Photochemical and Radiolytic Production of an Organic Hydride Donor with a Ru^{II} Complex Containing an NAD⁺ Model Ligand

The Ru-pbn complex with an NAD⁺/NADH model ligand, [Ru(bpy)₂(pbn)]²⁺ ([1]²⁺), which acts as a catalyst in the electrochemical reduction of acetone to 2-propanol, similar to the enzymatic NAD⁺/NADH. The complex [1]²⁺ undergoes the reversible pbn^{-•}/pbn redox reaction at -0.72, V versus SCE in CH₃CN, which shows pH dependent (59 mV/pH) between pH 2 and 11 in H₂O, indicating the occurrence of one-electron reduction coupled with a proton-transfer reaction. The excited state of [1]²⁺ was reductively quenched by an amine to produce the one-electron-reduced species in dry organic solvents. The one-electron-reduced species is a pbn ligand radical anion and is stable in CH₃CN. On the other hand, continuous photolysis (λ > 300 nm) of a CH₃CN/triethanolamine (TEOA) solution (4 : 1, v/v) containing [1](PF₆)₂ produced [(1)HH]²⁺ with a quantum yield of 0.21 at λ = (355 ± 6) nm. Single crystals of [(1)HH](PF₆)₂·2CH₃CN is similar to that of [1]²⁺ except for the pbn and pbnH₂ ligands. Elongation of the C8–C10 and C8–C12 bonds of [(1)HH]²⁺ (1.510(4) and 1.498(6)) compared with those of [1]²⁺ (1.376(10) and 1.399(9)) demonstrates the



Scheme 1. The mechanism for photochemical two-electron reduction of [1]²⁺.

formation of the 1,4-dihydropyridine framework in the pbnHH ligand (eq 2). Reduction of [1]²⁺ by $\text{CO}_2^{\bullet -}$ is first order in the concentration of [1]²⁺ and the protonation is very fast in a pH range from 3 to 13. A bimolecular decay of the transient species [(1)H]²⁺ reveals that the species reacts via disproportionation to form [1]²⁺ and [(1)HH]²⁺. Thus, the photochemical reduction of [1]²⁺ produces [(1)HH]²⁺ without accompanying undesirable carbon-centered radical–radical coupling of [1]⁺ or [H(1)]²⁺ radicals because of the steric interaction associated with the bulky {Ru(bpy)₂} moiety. The photochemical two-electron reduction of [1]²⁺ is reasonably explained by Scheme 1. The initial step is one-electron reduction of [1]²⁺ by $\text{CO}_2^{\bullet -}$ affording (2), and the following rapid protonation of the nitrogen atom (3). The resultant neutral pbnH[•] radical ligand (3) forms a π – π complex ((3)₂). The subsequent electron coupled proton transfer or hydrogen atom

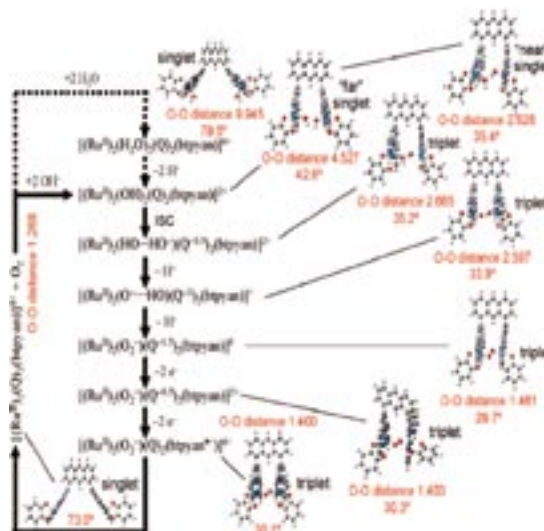


transfer from one neutral pbnH[•] to another one in the π – π complex produces the equimolar amount of [1]²⁺ and [(1)HH]²⁺. The finding of the photochemical two-electron reduction through disproportionation affording an equimolar amount of the oxide and two-electron reduced forms (Scheme 1) opens a new era for the photochemical multi-electron reduction of metal complexes, since the repeat of the photochemical two-electron reduction of the pbn moiety allowed smooth photochemical four-electron reduction of an analogous [Ru(bbnp)](trpy)]²⁺ (bbnp = 2,6-bis(benzo[b]-1,5-naphthyridin-6-yl)-4-*tert*-butylpyridine) under illumination of visible light in $\text{CH}_3\text{CN}/\text{TEOA}$ by (eq 3).

2. Water Oxidation by a Ruthenium Complex with Noninnocent Quinone Ligands: Possible Formation of an O–O Bond at a Low Oxidation State of the Metal

We have reported that a novel dinuclear Ru complex,

[Ru₂(OH)₂(3,6-Bu₂Q)₂(btpyan)](SbF₆)₂ (3,6-Bu₂Q = 3,6-ditertbutyl-1,2-benzoquinone, btpyan = 1,8-bis-(2,2':6',2''-terpyridyl)-anthracene), that contains redox active quinone ligands and has an excellent electrocatalytic activity for water oxidation (TON > 35000) when immobilized on an ITO electrode (*Inorg. Chem.* **40**, 329–337 (2001)). The novel features of the dinuclear and related mononuclear Ru species with quinone ligands, and comparison of their properties to those of the Ru analogues with the bpy ligand (bpy = 2,2'-bipyridine) replacing quinone, are discussed together with new theoretical and experimental results that show striking features for both the dinuclear and mononuclear species. The identity and oxidation state of key mononuclear species, including the oxyl radical, have been reassigned. Gas-phase theoretical calculations indicate that the Ru-dinuclear catalyst seems to maintain predominantly Ru(II) centers while the quinone ligands and water moiety are involved in redox reactions throughout the entire catalytic cycle for water oxidation. Theoretical study identifies [Ru₂(O₂⁻)(Q^{-1.5})₂(btpyan)]⁰ as a



Scheme 2. The mechanism of eight-electron of water catalyzed by a Ru dinuclear complex.

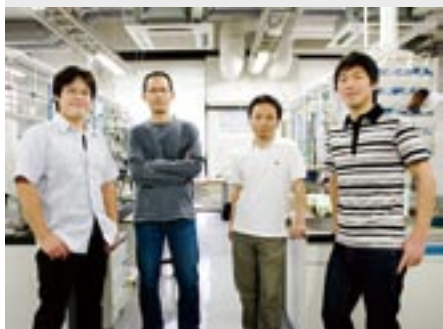
key intermediate and the most reduced catalyst species that is formed by removal of all four protons before four-electron oxidation takes place. The over all reaction mechanism for the four-electron oxidation of water catalyzed by the dinuclear Ru complex is shown in Scheme 2.

References

- (a) D. Polansky, D. Cabelli, J. Muckerman, E. Fujita, T. Koizumi, T. Fukushima, T. Wada and K. Tanaka, *Angew. Chem., Int. Ed.* **46**, 5728–5730 (2007). (b) H. Tannai, T. Koizumi and K. Tanaka, *Angew. Chem., Int. Ed.* **46**, 7112–7115 (2007).
- (a) T. Koizumi and K. Tanaka, *Angew. Chem., Int. Ed.* **44**, 5891–5894 (2005). (b) J. Muckerman, D. Polansky, T. Wada, K. Tanaka and E. Fujita, *Inorg. Chem.* **47**, 3958–3968 (2008).

Synthesis and Reactions of Transition Metal Complexes Having Aryloxy-Based Ligands, Especially with Regard to Activation of Small Molecules

Department of Life and Coordination-Complex Molecular Science
Division of Functional Coordination Chemistry



KAWAGUCHI, Hiroyuki
ISHIDA, Yutaka
WATANABE, Takahito
AKAGI, Fumio

Associate Professor*
Assistant Professor†
IMS Fellow‡
Post-Doctoral Fellow‡

This project is focused on the design and synthesis of new ligands that are capable of supporting novel structural features and reactivity. Currently, we are investigating multidentate ligands based on aryloxy and thiolate. In addition, we set out to study metal complexes with sterically hindered aryloxy and arylthiolate ligands. Our recent efforts have been directed toward activation of small molecules.

Development of ligands that play important roles in coordination chemistry has been the subject of intense interest. The chemistry of metal aryloxy complexes has shown that aryloxy ligands can promote various important transformations at metal centers. Therefore, aryloxy ligands complement the well-studied cyclopentadienyl-based systems, with the major difference being the greater reactivity of the aryloxy complexes due to their relatively higher unsaturation and lower coordination numbers for a $(\text{ArO})_n\text{M}$ fragment. However, coordinatively unsaturated metal complexes undergo facile ligand redistribution reactions, which are occasionally a severe obstacle to synthetic efforts.

One of strategies for overcoming this problem is the use of covalently linked ancillary ligands, thereby limiting ligand mobility and leaving little possibility to reorganize the molecule. This feature might lead to the isolation and structural characterization of a number of metal complexes that are difficult to obtain with aryloxy monodentate ligands.

1. Diniobium Tetrahydride Complex Bearing a Tripodal Triaryloxy Ligand¹⁾

We previously reported the synthesis of early transition metal hydride complexes supported by a linear triaryloxy ligand. As part of our studies of ancillary ligand effects, we recently began to study transition metal complexes with a tripodal triaryloxy ligand $[\text{O}_3]^{3-}$. The $[\text{O}_3]$ ligand provides a

rigid and facial donor environment. Herein, we were interested in extending this chemistry to niobium.

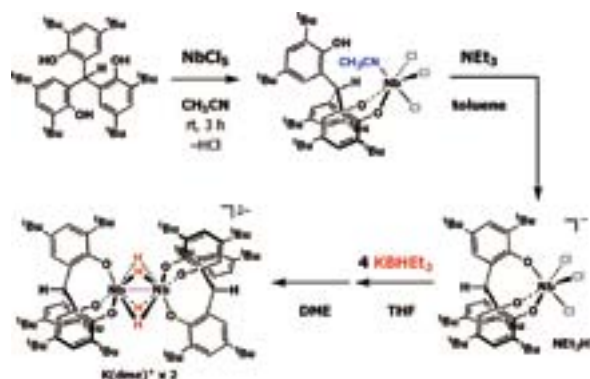


Figure 1. Synthesis of the hydride complex.

Treatment of NbCl_5 with the pro-ligand $\text{H}_3[\text{O}_3]$ in CH_3CN to give $\text{H}[\text{O}_3]\text{NbCl}_3(\text{CH}_3\text{CN})$ in 77% yield. The remaining hydroxy group in the nitrile adduct was deprotonated by NEt_3 in toluene at 80°C , yielding $[\text{NEt}_3\text{H}][(\text{O}_3)\text{NbCl}_3]$ as a red powder in 92%. An X-ray structure analysis of the trichloride complex reveals that the triaryloxy ligand coordinates to Nb facially.

Reaction of the trichloride complex with 4 equivalents of KBHET_3 in toluene/THF followed by recrystallization from DME gave yellow crystals of $[\text{K}(\text{dme})]_2\{[(\text{O}_3)\text{Nb}]_2(\mu\text{-H})_4\}$ in 66% yield along with evolution of H_2 . During the reaction, KBHET_3 partially acts as a reductant, and the metal center is reduced from Nb(V) to Nb(IV). The deuterated analogue was quantitatively prepared by treatment of the hydride complex under D_2 gas for three days at room temperature and was characterized by NMR spectroscopy.

An X-ray crystal structure determination of the hydride complex reveals a dimeric structure with two $[(\text{O}_3)\text{Nb}]$ frag-

ments bridged by four hydride ligands. The short Nb–Nb distance of 2.5690(5) Å indicates metal–metal bonding, thus accounting for the observed diamagnetism. The NMR spectra of the hydride complex are consistent with its solid-state structure if a fluxional process is invoked to explain the observed equivalence of the aryloxy groups on the NMR timescale at 25 °C. The bridging hydrides are observed as a broad signal at 6.29 ppm in the ^1H NMR spectrum. Upon cooling the sample, we did not detect any significant change in the hydride region.

2. Dinitrogen Activation by the Hydride Complex

Activation of molecular nitrogen by soluble metal complexes has attracted widespread attention from both fundamental and practical points of view. Dinitrogen cleavage by metal hydride complexes could be important in a catalytic system and is relevant to the Haber-Bosch process and a biological nitrogen-fixing system constituted by the metalloenzyme nitrogenase. Although late-transition-metal hydride complexes are often found to weakly bind dinitrogen with concomitant elimination of H_2 , conversion of an early-transition-metal hydride to a dinitrogen complex is a rarely documented phenomenon.

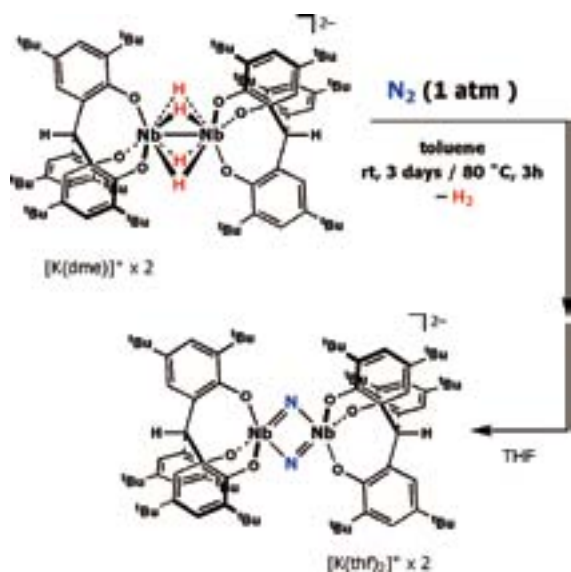


Figure 2. Reaction of the hydride complex with N_2 .

The dinioium tetrahydride complex appears to be thermally stable in solution under argon, while exposure of its toluene solution to an atmosphere of N_2 at room temperature resulted in a gradual color change from maroon to yellow brown for 3 days. Recrystallization from THF/pentane gave $[\text{K}(\text{thf})_2]_2[\{(\text{O}_3\text{Nb})_2(\mu\text{-N})_2\}]$ as yellow crystals in 37% yield.

The isotopically labeled complex was prepared analogously under $^{15}\text{N}_2$ and exhibits a single resonance at 311 ppm in the ^{15}N NMR spectrum. This result confirms that the origin of the nitride ligands is added N_2 . In the ^1H NMR spectrum, the nitride complex possesses high symmetry in solution, as equivalent aryloxy groups are observed.

An X-ray crystal structure determination of the nitride complex has shown it to be dimeric, constructed around a planar Nb_2N_2 four-membered ring that resides on a pseudo-two-fold axis. Reduction of dinitrogen by the hydride complex results in cleavage of the $\text{N}\equiv\text{N}$ bond, as evidenced by the N–N separation of 2.589(5) Å. Each niobium center displays five-coordinate, distorted trigonal-bipyramidal coordination.

The nucleophilic behavior of the nitride groups was observed in the reaction with methyl iodide. The nitride complex was treated with excess of methyl iodide at room temperature to afford $[\text{K}(\text{thf})][\{(\text{O}_3\text{Nb})_2(\mu\text{-N})(\mu\text{-NMe})\}]$. When the reaction mixture was carried out at 60 °C for 5 days, the remaining nitride was methylated, giving a bis-imide complex $[\{(\text{O}_3\text{Nb})_2(\mu\text{-NMe})_2\}]$.



Figure 3. Reaction of the nitride complex with MeI.

Reduction of N_2 utilizing the hydride complex as described here is closely related to work by Fryzuk *et al.*, who used the tantalum(IV) hydride complex $[\{(\text{NPN})\text{Ta}\}_2(\mu\text{-H})_4]$ ($[\text{NPN}] = \text{PhP}(\text{CH}_2\text{SiMe}_2\text{NPh})_2$). This complex was found to react with N_2 through partial loss of H_2 to give the dinitrogen complex $[\{(\text{NPN})\text{Ta}\}_2(\mu\text{-}\eta^1\text{:}\eta^2\text{-N}_2)(\mu\text{-H})_2]$, in which two hydride ligands remain coordinated. Subsequent treatment with boranes, silanes, and zirconium hydrides resulted in N_2 triple bond cleavage of the coordinated N_2 molecule. In our case, the cleavage proceeded spontaneously and did not require external reducing agent. This process corresponds to an overall six-electron reduction of N_2 , in which two electrons are initially stored in a metal–metal bond, and four additional electrons are provided by H_2 elimination.

Reference

- 1) F. Akagi, T. Matsuo and Y. Ishida, *Angew. Chem., Int. Ed.* **46**, 8778–8781 (2007).

* Present Position; Professor, Department of Chemistry, Tokyo Institute of Technology, Ookayama, Meguro-ku, Tokyo 152-8551

† Present Address; Department of Chemistry, Tokyo Institute of Technology, Ookayama, Meguro-ku, Tokyo 152-8551

‡ Present Address; Department of Materials Science and Environmental Engineering, Tokyo University of Science, Yamaguchi, Sanyo-onodashi, Yamaguchi 756-0884

Visiting Professors



Visiting Professor
ITOH, Shinobu (*from Osaka University*)

Dioxygen Activation Mechanism by Copper Proteins and Their Models

The structure and reactivity of copper/active-oxygen complexes have attracted much interest during the past decades because of their potential relevance to biological systems and numerous copper-catalyzed oxidation reactions. In our laboratory, we have been studying the reactivity of several types of copper/active-oxygen species such as mononuclear and dinuclear copper(II)-peroxo and copper(III)-oxo complexes in order to evaluate the catalytic mechanism of copper oxygenases and to develop efficient oxidation catalysts for organic synthesis.



Visiting Associate Professor
HASEGAWA, Miki (*from Aoyama Gakuin University*)

Development of Lanthanide Complexes with Novel Optical Properties by the Coordination Chemistry

The 4f-electrons of the lanthanides, which are the key to developing functional molecules such as molecular magnets and emissive compounds, are shielded by the 5d and 6s orbitals. The interrelation of molecular design and functionality has not been established yet, because the electronic structure of f-elements is more complicated than that of d-block ions. Coordination chemistry is useful in this context. For instance, we succeeded in manipulating the ff-emission selectively by tuning the energy state of the ligand with some substituents. In addition, molecular arrangements on ultra-thin films have been used to induce polarized optical behavior. These approaches are based on our concepts to develop high-efficient optical materials under a scientific strategy. The ff-transitions of lanthanide complexes can be observed easily, but the underlying theory is not sufficient yet. We are ambitious to control the optical functionality of lanthanide ions with the help of coordination chemistry.



Visiting Associate Professor
TAKAHASHI, Satoshi (*from Osaka University*)

Dynamics of Protein Folding by Single Molecule and Ensemble Techniques

Protein is a linear macromolecule that has a unique property to fold to a specific three-dimensional structure from fully unfolded conformations. We are interested in the physical principles that connect the unfolded and the folded conformations of proteins. To detect fast kinetic processes involved in protein folding, we use rapid mixing device for the time resolved observation of average protein structures. To observe heterogeneity and dynamic fluctuations, we use single molecule observation systems. Based on the ensemble measurements on several proteins using small angle X-ray scattering and circular dichroism spectroscopy, we proposed “collapse and search” mechanism of protein folding. The recent application of single molecule fluorescence measurements clarified a relatively slow conformational dynamics in the unfolded state. We are hoping to obtain important information required for the protein structure prediction and design through the further examination of protein folding dynamics.